Characterisation of Roman copper alloy artefacts and soil from Rakafot 54 (Beer Sheva, Israel)

2019 IMEKO TC-4 International Conference on
Metrology for Archaeology and Cultural Heritage
Florence, Italy, December 4-6, 2019

Characterisation of Roman copper alloy artefacts and soil from Rakafot 54 (Beer Sheva, Israel)

Manuel J.H. Peters[1,2,3], Yuval Goren[3], Peter Fabian[3], José Mirão[2],
Sabrina Grassini[1], Emma Angelini[1]

[1] Department of Applied Science and Technology, Politecnico di Torino,
Corso Duca degli Abruzzi 24, 10129 Torino, Italy,
manuel.peters@polito.it; sabrina.grassini@polito.it; emma.angelini@polito.it
[2] HERCULES Laboratory, Department of Geosciences, Universidade de Évora,
Rua Romão Ramalho 59, 7000-671 Évora, Portugal, jmirao@uevora.pt
[3] Department of Bible, Archaeology & Ancient Near East, Ben-Gurion University of the Negev
P.O.B. 653 Beer-Sheva 8410501, Israel, ygoren@bgu.ac.il; fabian@bgu.ac.il

Abstract –
The research presented in this paper focused on the preliminary non-destructive analysis of copper alloys, corrosion, and soil components from a Roman archaeological site in Israel. pXRF, XRD, and micromorphological analyses were carried out to gain a better understanding of the corrosion processes affecting the copper alloy artefacts, by characterising the alloy composition, soil environments, and corrosion products. Preliminary results indicate that the artefacts consist of copper-lead-tin alloys, covered by copper hydroxy-chlorides and lead sulphate phases with slight variations in their crystallisation. The multi-analytical approach revealed the presence of quartz, calcite, gypsum and feldspars in the sediments, while thin sections more specifically indicate loess soils with local micro-environments.

I. INTRODUCTION

Understanding the degradation processes of metallic artefacts is of importance in order to design a proper strategy for conservation treatment and storage. Within the same archaeological site, similar artefacts can have significantly different states of preservation, often related to variations in environmental parameters such as local soil conditions [1]. The present research investigates this topic by analysing various copper alloy artefacts from an arid site on the edge of the Negev desert in Israel (Fig. 1). Rakafot 54 was excavated during two seasons in 2018 and 2019 as a collaboration between the Israel Antiquities Authority and Ben-Gurion University of the Negev. The site was probably established during the first century CE and demolished during the Bar Kochba revolt against Rome (132-135/6 CE). Several indications of regular habitation have been found, including oil lamp fragments and limestone vessels. The site is placed near the border between Judea and Nabataea, close to a Roman road, and includes a watchtower, hearths, garbage pits, and an underground system. Numerous metallic objects were found during the excavations, including copper alloy coins minted by Herod Agrippa I (ruled 41-44 CE) and the Roman procurators in Judaea (6-66 CE). Additionally, provincial Roman coins minted in Ashkelon during the reign of Nero to Trajan (37-117 CE), Nabataean coins (until 106 CE) and coins of The First Jewish–Roman War (66–73 CE) were found.

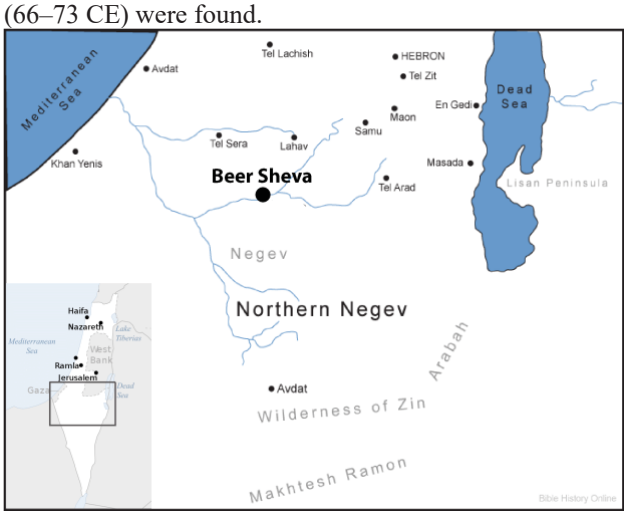

Fig. 1. Location of the site (at the city of Beer Sheva).

In terms of the geological setting, the site is located on quaternary alluvium loess soil. The loess is soft yellow windblown silty sediment, dominated by quartz silt, clay and calcite. The loess deposition, by southern-western winds from Sinai and North Africa, started at the end of the Pleistocene and continues into the Holocene. The loess formation is bordered to the west by a coastline of calcareous sandstone and sand dunes, to the south by sand dunes, to the east by Eocene Adulam formation which is mainly chalk and chert, and to the north by quaternary red sand and loam (locally termed Hamra soil) [2]. In the Beer

Sheva area, where mean annual precipitation is 200–350 mm, loess covers the entire landscape and pre-existing topography [3].

The soil components of the archaeological site are largely dependent on the general geological setting, with local variations due to anthropogenic activities and post-depositional processes. These variations could possibly lead to micro-environments corresponding to the various excavation loci. The copper alloy objects coming from the site were covered with a heterogeneous layer of corrosion products and sediment (Fig. 2). The items were retrieved from different areas, which contained sediments that indeed appeared to have distinctively different compositions, based on a visual inspection. This could possibly affect the corrosion process in various ways. In order to gain a better understanding of both the degradation processes affecting these artefacts and to determine their state of preservation and possible future steps for conservation, a selection of artefacts was analysed with portable X-ray fluorescence (pXRF) and X-ray diffraction (XRD). The reason behind this approach lies in the general need to avoid intrusive sampling of museum objects and the requirement for the exclusive application of non-destructive testing (NDT) techniques for the material characterisation of cultural artefacts. As a result, research is gradually becoming reliant on portable instrumentation (e.g., pXRF) that, in the NDT mode, is intended to screen only the surfaces of the objects under investigation. However, especially in the case of metals, the effects of chemical-physical processes responsible for degradation and corrosion as well as surface enrichment or loss of elements make NDT highly problematic. Although the degradation processes of metallic artefacts are well-known and widely investigated, every artefact has a specific history strictly related to its depositional micro-environment [1]. The environmental parameters influence the corrosion process and affect the various areas of the metallic objects differently. Consequently, it is of high importance to assess the specific deterioration of the artefacts in order to be able to interpret the results of NDT surface investigation. This paper describes the preliminary steps of the ongoing research and proposes some directions for future research.

Fig. 2. Copper alloy coin with corrosion and soil.

II. DATA

This research investigated the alloys, corrosion products, and related soil of a group of corroded metallic artefacts from Rakafot 54, including coins and other objects. During the excavation, the location of the metallic artefacts was recorded by assigning them to the specific locus they originated from, and the same was done for the soil samples. In this paper, several artefacts and soil samples that have a clear connection were considered. An overview of the sample types, analytical techniques and the expected information can be found in Table 1.

Table 1. Sample types and analytical techniques.

Sample type	Technique	Information
Artefact surface	pXRF	Alloy & soil
Corrosion powder	XRD	Corrosion & soil
Soil thin section	Petrography	Soil

III. METHODS

A preliminary pXRF surface screening was carried out on the coins prior to conservation treatment, in order to determine the major alloy components of the coins (Fig. 3). A Thermo Scientific Niton XL3t GOLDD+ XRF Analyser equipped with a Geometrically Optimized Large Area Drift Detector and 50 kV, 200 μA Ag anode was used, with an 8 mm collimator. The data was obtained with the Cu/Zn mining measurement mode, using 120 seconds scanning time. Both sides of each coin were measured.

Fig. 3. Coin positioned for pXRF analysis.

XRD measurements were performed separately on the corrosion samples collected from the artefacts. Sampling was done by carefully removing a portion of corrosion from the objects with a scalpel, paying attention to not damage the *limitos* (the surface boundary between the external corrosion products and the corrosion that has

replaced the bulk metal, isomorphic with the uncorroded artefact). The samples were then homogenised using an agate mortar and a few drops of ethanol. This emulsion was positioned in the middle of a zero-background silicon sample holder and flattened, after which the ethanol was left to evaporate (Fig. 4). Diffractograms were taken from the samples with a PANalytical X'Pert Pro powder X-ray diffractometer equipped with PIXcel 1D detector and a Cu K-alpha source with wavelength 1.54 Å, at 40 kV with a current of 40 mA.

Fig. 4. Corrosion sample on sample holder.

Thin sections from the soil samples were obtained by embedding a portion of each sample in epoxy resin, mounting it on a glass microscope slide, and grinding and polishing it to 30 µm (Fig. 5). The thin sections were then observed with a petrographic microscope under polarised light.

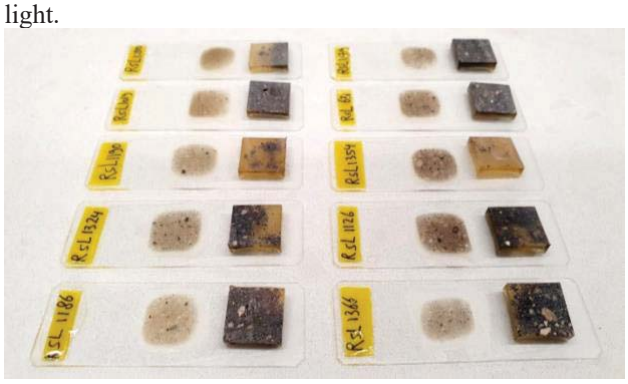

Fig. 5. Soil thin sections.

IV. RESULTS

The obtained results will be briefly described according to their analytical method, after which they will be combined and elaborated in the discussion.

A. pXRF

The preliminary pXRF screening of the coins indicates that most of the objects are made of copper-lead-tin alloys, with relatively high amounts of lead (Table 2). The presence of silver is always below the limit of detection, and zinc appears to be only present as trace element in some cases. There are inconsistencies between the measurements on the obverse (a) and reverse (b) sides of each coin, probably stemming from the position of the samples on the instrument, and the fact that these measurements were carried out on uncleaned objects. Consequently, the results are largely dependent on the corrosion layers and sediments present on the surface. Nevertheless, these results offer a useful indication of the primary alloy components of the coins found at the site and offer a clue of the possible corrosion products.

Table 2. Primary alloy components (pXRF).

Sample	Cu	Pb	Sn	Zn	Ag
B6058a	46.8	5.1	2.7	0.04	< 0.03
B6058b	45.1	5.7	1.0	< 0.03	< 0.03
B6081a	44.6	13.0	3.4	< 0.05	< 0.04
B6081b	47.5	5.6	0.45	< 0.03	< 0.03
B6101a	42.1	6.8	1.5	< 0.04	< 0.03
B6101b	36.0	14.4	4.4	< 0.04	< 0.04
B8103a	43.0	1.1	0.04	< 0.04	< 0.02
B8103b	36.0	3.4	2.1	0.02	< 0.02
B8764a	43.9	3.2	0.34	0.03	< 0.02
B8764b	46.5	3.0	2.6	0.05	< 0.03
B9803a	44.0	5.1	1.3	< 0.03	< 0.02
B9803b	32.1	14	5.0	< 0.04	< 0.04

Additionally, the pXRF measurements provide information about the traces of sediments that are possibly present on the surface of the artefacts together with the formed corrosion phases (Table 3). Significant amounts of calcium, chlorine and silicon can be observed as well as smaller amounts of aluminium, potassium, and sulphur. Additional components can be found in Table 4.

Table 3. Soil components on artefact surface (pXRF).

Sample	Al	Ca	Cl	K	S	Si
B6058a	2.1	8.7	4.61	0.25	1.12	9.1
B6058b	2.3	4.9	5.09	0.38	1.52	13.1
B6081a	1.4	5.4	5.77	0.11	3.81	4.7
B6081b	0.9	2.9	9.9	0.15	2.18	3.2
B6101a	2.1	6.0	5.46	0.35	2.20	9.1
B6101b	1.0	10.1	3.22	0.20	3.44	9.1
B8103a	1.9	7.4	3.67	0.31	0.55	11.9
B8103b	1.6	8.4	1.27	0.34	1.42	13.4
B8764a	1.9	4.9	8.0	0.32	1.66	7.4
B8764b	1.7	10.6	6.27	0.26	1.33	6.0
B9803a	2.7	10.7	4.33	0.39	1.13	11.5
B9803b	3.2	13.9	2.34	0.70	1.35	12.5

Table 4. Trace elements on artefact surface (pXRF).

Sample	Fe	Mg	Mn	Ni	P	Ti
B6058a	0.51	< 2.4	< 0.02	0.02	0.11	0.11
B6058b	0.81	< 3.4	< 0.03	0.02	0.16	0.17
B6081a	0.13	< 2.6	< 0.02	0.04	0.80	0.04
B6081b	0.34	< 3.1	< 0.02	0.01	0.07	0.05
B6101a	0.68	2.6	< 0.03	< 0.02	0.29	0.13
B6101b	0.33	2.9	0.02	0.01	0.60	0.06
B8103a	0.59	< 4.0	< 0.02	< 0.02	0.31	0.11
B8103b	0.77	< 4.4	< 0.02	< 0.02	0.46	0.17
B8764a	0.60	< 4.0	< 0.02	0.03	0.29	0.12
B8764b	0.51	< 4.4	< 0.02	0.02	0.08	0.09
B9803a	0.56	< 2.4	< 0.03	< 0.02	0.14	0.12
B9803b	1.25	< 2.0	0.03	0.02	0.28	0.23

B. Micromorphology

In the thin sections and under the petrographic microscope, all soil samples reveal a matrix that is silty and somewhat highly calcareous. The silt is well-sorted and contains mainly quartz, but also a recognisable quantity of other minerals, including hornblende, zircon, mica minerals, feldspars, tourmaline, augite and more rarely garnet, epidote and rutile. Ore minerals are abundant too in this fraction. The sand fraction includes dense, well sorted, rounded sand-sized quartz grains, and limestone. Based on a bulk of published data it is readily identified as loess soil [4]. However, micromorphological features within this given theme indicate more specific micro-environments, resulting from an array of anthropogenic activities as well as post-depositional processes.

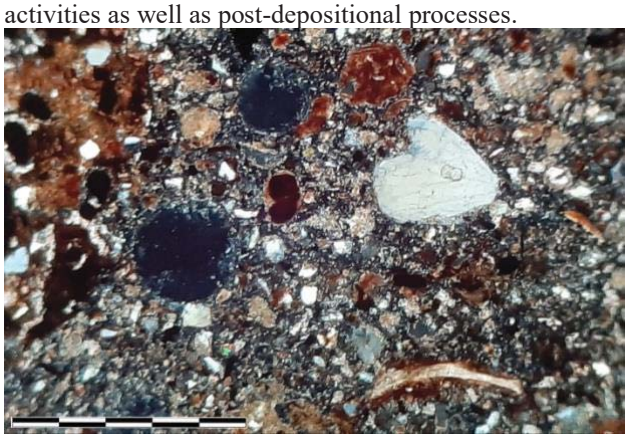

Fig. 6. View of soil sample RSL1126 in thin section under the microscope, crossed polarisers. The matrix is silty and calcareous. An aeolian quartz sandy grain is seen to the right. Charred ash material is seen as opaque bodies. Snail fragment in the bottom right. Burnt soil with ferric corrosion products are seen at the left. Bar size: 1 mm.

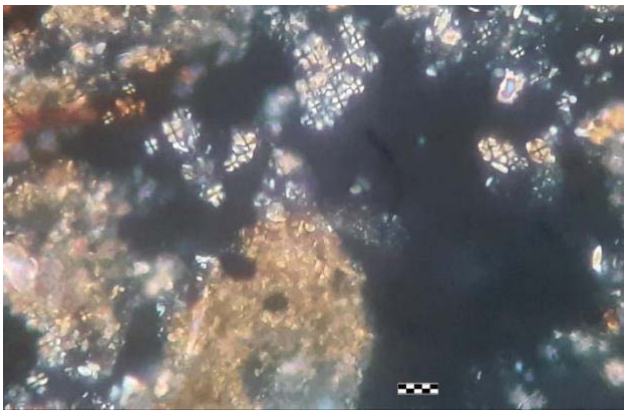

Fig. 7. View of soil sample RSL1354 in thin section under the microscope, crossed polarisers, showing a concentration of herbivore dung spherulites in anthropogenic ash layer from a hearth. Bar size: 10 μm.

The post-depositional processes are reflected by re-crystallisation of calcite and gypsum from ground water, corrosion products of metals (Fig. 6), mineral replacements, clay relocation etc. Anthropogenic features include remnants of human activities such as slag, coprolites (Fig. 7), pottery and brick crumbs, charred plant remains, phytolith concentrations and other ash characteristics, and more. All these will be used in further research to define the immediate micro-environmental physiognomies of the sediment at the immediate proximity of each artefact, in order to correlate it with the corrosion composition.

C. XRD

A typical XRD diffractogram which includes most of the peaks representative for these samples is shown in Fig. 8. Although there are some visual differences in the diffractograms, mainly related to variations of peak intensities, the main components appear to be relatively consistent.

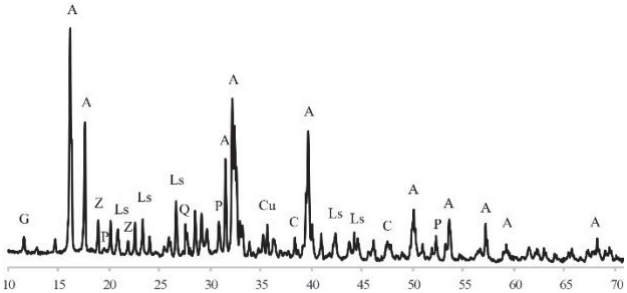

Fig. 8. Representative diffractogram of corrosion sample RCB9803 (connected to soil sample RSL1354), depicting the most common mineral phases identified in the samples. A=atacamite; Cu=cuprite; Ls=lead sulphate; C=calcite; Q=quartz; G=gypsum; Z=zeolite; P=paratacamite.

The primary compound in all samples was identified as atacamite ($Cu_2(OH)_3Cl$), the orthorhombic phase of copper

hydroxy-chloride, which can be commonly found on copper alloy archaeological objects extracted from salty soils [5]. Clinoatacamite, its monoclinic polymorph, has been detected in two samples, while its presence is not clear in the rest of the cluster under investigation. Paratacamite ($Cu_3(Cu,Zn)(OH)_6Cl_2$), a zinc-enriched variety of the copper hydroxy-chloride series, also appears in the majority of the diffractograms. Even though it is not considered a polymorph, it is still closely related to atacamite as part of the degradation process [6]. Lead sulphate was identified in most samples, while cuprite was identified in all samples except for RCB6081. This exception might be related to inconsistencies in sampling depth.

All diffractograms reveal the persistent presence of quartz, which can be explained by the traces of sediment that were present on the surface of the artefacts during the sample preparation for the XRD analyses. Other soil components that were identified in this step are K- and Na-based feldspars (albite and orthoclase), together with clay minerals such as zeolite. Gypsum and its polymorphs were identified in RCB6058, RCB6101, and RCB9803, but may also be present in other samples.

D. Discussion

In order to validate the results of the individual techniques, several comparisons were made. The identification of atacamite in the diffractograms can be correlated with the presence of Cl in the pXRF results. It is still unclear whether this presence is related to the hydroxy-chloride phases of the corrosion, or to another Cl-based mineral present in the soil. Differentiating between the lead sulphate and calcite peaks in the XRD diffractograms was complicated in some cases, however, a clear correlation could be observed between the presence of sulphur and significant amounts of lead in the pXRF data, and the presence of lead sulphate in the diffractograms. Although the presence of tin is clear in the primary alloy identification with pXRF, no tin-based corrosion products were identified in the diffractograms; however, tin oxides are reported to provide difficulties in identification with XRD [7, 8, 9]. The Si presence in the pXRF data could be related to the quartz observed in the diffractograms and the thin sections. The K and Si combination could be explained as K-based feldspars and quartz with the diffractograms, and similarly, Si and Al could be identified together as feldspars and clay minerals.

Most minerals identified in the micromorphological study of the thin sections have their origins in igneous or metamorphic rocks. Furthermore, the micromorphological study provides a description of the soil components that corresponds with the results from the pXRF and XRD analyses.

V. CONCLUSIONS

The overarching purpose of this research was to obtain a better understanding of the various factors influencing the degradation of a set of Roman artefacts coming from Rakafot 54 in Israel, by using a multi-analytical approach that relied on elemental, mineralogical, and petrographic characterisation.

The first objective was to identify the main alloy components. This was accomplished by carrying out a preliminary pXRF screening on the artefact surfaces before cleaning, which showed that the alloys were all copper-lead-tin based.

The second goal of this research was the determination of possible corrosion products of the objects, which was done by carrying out XRD analysis on small corrosion powder samples. The results here indicate a strong presence of copper hydroxy-chlorides such as atacamite and clinoatacamite. Paratacamite was also detected in the majority of the samples and finds partial confirmation in the detection of small amounts of Zn with pXRF. Additionally, some lead sulphates were detected, which could be correlated with the elemental data.

Finally, the main soil components were identified. By combining pXRF, XRD, and micromorphology, it was shown that the soil mainly consists of quartz, calcite, feldspars, clay minerals, and gypsum.

Although the micromorphological study indicates local differences in soil components of the various samples, often related to burning and organic materials (presence of phytoliths and spherulites), these differences do not appear to have a clear effect on the corrosion products. The differences in intensities of the diffraction peaks representing the various corrosion compounds, and the absence of cuprite in one sample could be related to inconsistencies in sampling depth and small sample size. Additionally, it is possible that some soil features, such as the presence of chlorides, negate the effect that small variations in soil and alloy components could have.

While there are several limitations to this research, mostly resulting from the relatively small amounts of corrosion available for analysis, the presented results provide interesting directions for future research, which will focus more strongly on investigating the relationship between the soil conditions and corrosion products. This could be done by carrying out SEM and micro-Raman analysis on the corroded surface of the coins, pXRF measurements on the bulk metal below the corroded surface, and further analysis of the various soil components by methods such as XRD.

VI. ACKNOWLEDGEMENTS

The authors would like to thank Mafalda Costa and Dulce Valdez for their assistance in the interpretation of the diffractograms and Silvia Bottura Scardina for her valuable comments. The research presented in this paper was carried out mainly using data collected at Politecnico

di Torino, Ben-Gurion University of the Negev, and Universidade de Évora, as part of H2020-MSCA-ITN-2017, ED-ARCHMAT (ESR7). This project has received funding from the European Union's Horizon 2020 research and innovation programme under the Marie Skłodowska-Curie grant agreement No 766311.

REFERENCES

[1] E.Angelini, F.Rosalbino, S.Grassini, G.M.Ingo, T.De Caro, "Simulation of corrosion processes of buried archaeological bronze artefacts", in P.Dillmann, G.Béranger, P.Piccardo, H.Matthiesen (eds), Corrosion of Metallic Heritage Artefacts: Investigation, Conservation and Prediction for Long-Term Behaviour, European Federation of Corrosion Publication 48, Woodhead Publishing, Cambridge, UK, 2007, pp.203–218.

[2] A.Sneh, and M.Rosenaft, "Geological Map of Israel 1:50,000, Sheet 14-1: Netivot", Jerusalem, 1994.

[3] O.Crouvi, R.Amit, M.Ben Israel, Y.Enzel, "Loess in the Negev Desert: Sources, Loessial Soils, Palaeosols, and Palaeoclimatic Implications", in Y.Enzel and O.Bar-Yosef (eds), Quaternary of the Levant, Environments, Climate Change, and Humans, Cambridge, UK, 2017, pp.471-482.

[4] Y.Goren, I.Finkelstein, N.Na'aman, "Inscribed in Clay: Provenance Study of the Amarna Tablets and Other Ancient Near Eastern Texts", Tel Aviv. 2004, pp.112-113 with references.

[5] A.G.Nord, E.Mattson, K.Tronner, "Factors Influencing the Long-Term Behavior of Bronze Artefacts in Soil", Protection of Metals, vol.41, 2005, pp.339-346.

[6] R.Frost, "Raman Spectroscopy of Selected Copper Minerals of Significance in Corrosion", Spectrochimica acta. Part A, Molecular and biomolecular spectroscopy, vol.59, 2003, pp.1195-1204.

[7] O.Oudbashi, "Multianalytical study of corrosion layers in some archaeological copper alloy artefacts", Surface and Interface Analysis, vol.47, 2015, pp.1133-1147.

[8] L.Robbiola, J.M.Blengino, C.Fiaud, "Morphology and Mechanisms of Formation of Natural Patinas on Archaeological Cu-Sn Alloys", Corrosion Science, vol.40, 1998, pp.2083-2111.

[9] P.Piccardo, B.Mille, L.Robbiola, "Tin and copper oxides in corroded archaeological bronzes', in P.Dillmann, G.Béranger, P.Piccardo, H.Matthiesen (eds), Corrosion of Metallic Heritage Artefacts: Investigation, Conservation and Prediction for Long-Term Behaviour, European Federation of Corrosion Publication 48, Woodhead Publishing, Cambridge, UK, 2007, pp.239–262.